Insights into the Molecular Determinants of Substrate Specificity in Glycoside Hydrolase Family 5 Revealed by the Crystal Structure and Kinetics of Cellvibrio mixtus Mannosidase 5A

Fernando M V Dias, Florence Vincent, Gavin Pell, José a M Prates, Maria S J Centeno, Louise E Tailford, Luís M A Ferreira, Carlos M G A Fontes, Gideon J Davies, Harry J Gilbert

THE JOURNAL OF BIOLOGICAL CHEMISTRY
Vol. 279, No. 24, Issue of June 11, pp. 25517–25526, 2004

Printed in U.S.A.

Insights into the Molecular Determinants of Substrate Specificity in Glycoside Hydrolase Family 5 Revealed by the Crystal Structure and Kinetics of *Cellvibrio mixtus* Mannosidase 5A*[S]

Received for publication, February 13, 2004, and in revised form, March 9, 2004
Published, JBC Papers in Press, March 10, 2004, DOI 10.1074/jbc.M401647200

Fernando M. V. Dias‡§, Florence Vincent§¶, Gavin Pell‖, José A. M. Prates‡, Maria S. J. Centeno‡, Louise E. Tailford‖, Luís M. A. Ferreira‡, Carlos M. G. A. Fontes‡, Gideon J. Davies¶, and Harry J. Gilbert‖‡‡**

From the ‡CIISA-Faculdade de Medicina Veterinária, Universidade Técnica de Lisboa, Rua Prof. Cid dos Santos, 1300-477 Lisboa, Portugal, the ¶Structural Biology Laboratory, Department of Chemistry, University of York, Heslington, York YO10 5YW, United Kingdom, and the ‖School of Cell and Molecular Biosciences, University of Newcastle upon Tyne, Newcastle upon Tyne, NE1 7RU, United Kingdom

The enzymatic hydrolysis of the glycosidic bond is central to numerous biological processes. Glycoside hydrolases, which catalyze these reactions, are grouped into families based on primary sequence similarities. One of the largest glycoside hydrolase families is glycoside hydrolase family 5 (GH5), which contains primarily endo-acting enzymes that hydrolyze β-mannans and β-glucans. Here we report the cloning, characterization, and three-dimensional structure of the *Cellvibrio mixtus* GH5 β-mannosidase (*Cm*Man5A). This enzyme releases mannose from the nonreducing end of mannooligosaccharides and polysaccharides, an activity not previously observed in this enzyme family. *Cm*Man5A contains a single glycone (−1) and two aglycone (+1 and +2) sugar-binding subsites. The −1 subsite displays absolute specificity for mannose, whereas the +1 subsite does not accommodate galactosyl side chains but will bind weakly to glucose. The +2 subsite is able to bind to decorated mannose residues. *Cm*Man5A displays similar activity against crystalline and amorphous mannans, a property rarely attributed to glycoside hydrolases. The 1.5 Å crystal structure reveals that *Cm*Man5A adopts a $(\beta/\alpha)_8$ barrel fold, and superimposition with GH5 *endo*-mannanases shows that dramatic differences in the length of three loops modify the active center accessibility and thus modulate the specificity from endo to exo. The most striking and significant difference is the extended loop between strand β8 and helix α8 comprising residues 378–412. This insertion forms a "double" steric barrier, formed by two short β-strands that function to "block" the substrate binding cleft at the edge of the −1 subsite forming the "exo" active center topology of *Cm*Man5A.

The plant cell wall represents the major source of organic carbon within the biosphere. The polysaccharides contained within these composite structures are hydrolyzed by an extensive repertoire of glycoside hydrolases, and the sugars released are then utilized as carbon and energy sources by a range of organisms. Mannose-containing polysaccharides are an important component of the plant cell wall and are present mainly as galactomannans in which the β1,4-linked mannopyranoside backbone is decorated with galactosyl residues at the O-6 position and glucomannan that contains a heterogeneous backbone of β1,4-linked glucose and mannose sugars (1) (Fig. 1). The polymeric backbone of these polysaccharides is hydrolyzed by endo-β-1,4-mannanases (hereafter "mannanase" (2), whereas the side chains of galactomannan are removed by α-galactosidases (3). The mannooligosaccharides generated by these enzymes are further hydrolyzed by β-mannosidases (EC 3.2.1.25), which are exo-acting glycoside hydrolases that catalyze the removal of the nonreducing end β-D-mannose (2). In the sequence-based classification of glycoside hydrolases (4, 5)[1] endo-mannanases are found in families GH5[2] and GH26 with β-mannosidases located in families GH1 and GH2.

Although mannanases have been extensively characterized, the precise catalytic profile of β-mannosidases is less clear. The GH1 and GH2 β-mannosidases hydrolyze glycosidic bonds by a double displacement mechanism leading to retention of anomeric configuration (6) and, based on conservation of the protein fold within a family, are predicted to adopt a $(\beta/\alpha)_8$ barrel structure, with the catalytic acid-base and nucleophile glutamates on β-strands 4 and 7, respectively (7). Indeed this view is supported by the identification of Glu^{429} and Glu^{519} as the catalytic acid-base and nucleophile, respectively in β-mannosidase 2A from *Cellulomonas fimi* (8, 9). The designation of enzymes as β-mannosidases is based primarily on their capacity to hydrolyze aryl-β-mannosides. There is, however, a paucity of information on the specificity for the aglycone region of the target substrates. The exo-β-mannanase from guar seeds hydrolyzes mannopentaose eight times faster than mannobiose pointing to productive binding of mannose residues at a minimum of two aglycone subsites (2, 10), whereas the β-mannosidase from *Helix pomatia* displays similar activity against manooligosaccharides with degrees of polymerization (d.p.)

* This work was supported in part by grants from the Biotechnology and Biological Sciences Research Council and the Wellcome Trust. The costs of publication of this article were defrayed in part by the payment of page charges. This article must therefore be hereby marked "*advertisement*" in accordance with 18 U.S.C. Section 1734 solely to indicate this fact.

[S] The on-line version of this article (available at http://www.jbc.org) contains supplemental material.

The atomic coordinates and structure factors (code 1uuq) have been deposited in the Protein Data Bank, Research Collaboratory for Structural Bioinformatics, Rutgers University, New Brunswick, NJ (http://www.rcsb.org/).

§ These authors contributed equally to this work.
** Royal Society University Research Fellow.
‡‡ To whom correspondence should be addressed. E-mail: h.j.gilbert@ncl.ac.uk.

[1] afmb.cnrs-mrs.fr/CAZY/.

[2] The abbreviations used are: GH, glycoside hydrolase family; d.p., degree(s) of polymerization; *Cm*Man5A, *C. mixtus* GH5 β-mannosidase; SAD, single-wavelength anomalous dispersion; HPLC, high pressure liquid chromatography; ITC, isothermal titration calorimetry.

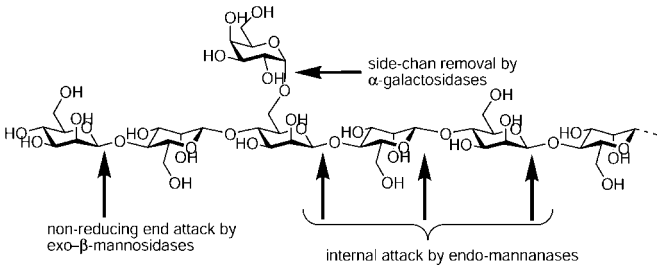

FIG. 1. **Schematic representation of galactomannan and the enzymes involved in its degradation.**

ranging from 2 to 5 (11). The capacity of these enzymes to hydrolyze oligosaccharides released from glucomannan is unknown. Furthermore, because the crystal structure of a β-mannosidase has not been reported, the molecular determinants that confer exo-mannanase activity are unknown.

Here we report the cloning, biochemical properties, and crystal structure of an exo-acting mannanase from *Cellvibrio mixtus* designated β-mannosidase 5A (*Cm*Man5A). Unlike all previously reported β-mannosidases, *Cm*Man5A is found in GH5. The enzyme contains one glycone site that confers tight specificity for *manno*-configured substrates and two aglycone binding sugar-binding sites. The 1.5 Å crystal structure of the enzyme, determined by single-wavelength anomalous dispersion (SAD) methods, reveals the structural basis for the exo-activity of *Cm*Man5A; extended loops and a tryptophan residue impose a steric block at the edge of the −1 subsite, preventing substrate access to the distal glycone-binding sites.

EXPERIMENTAL PROCEDURES

Bacterial Strains, Plasmids, and Culture Conditions—C. mixtus (NCIMB 8633) was cultured aerobically at 20 °C in Dubos mineral salts medium or on Dubos agar plates overlaid with filter paper (12). After autoclaving, the media were supplemented with sterile glucose (0.25%). *Escherichia coli* XL1-Blue (Stratagene) was cultured at 37 °C in LB or on LB-agar plates. The media were supplemented with 100 μg ml^{-1} ampicillin or 2 μg ml^{-1} 5-bromo-4-chloro-3-indolyl β-D-galactoside to select for *E. coli* transformants and recombinants, respectively. *E. coli* cells used to propagate bacteriophage were grown on LB supplemented with 10 mM $MgSO_4$ and 0.2% maltose and were plated out on NZYM top agar (0,7%). The bacteriophages and plasmids employed in this work were λZAPII (Stratagene), pBluescript SK$^-$ (Stratagene), pGEM T-easy (Promega), and pET21a (Novagen). The recombinant β-mannosidase was expressed in *E. coli* BL21 (DE3; Novagen) containing a derivative of pET21a encoding *Cm*Man5A and was cultured as described below.

General Recombinant DNA Procedures—Transformation of *E. coli*, agarose gel electrophoresis, Southern hybridization, slot blot hybridizations, plaque hybridizations, and the general use of nucleic acid modifying enzymes were as described by Sambrook *et al.* (13). Plasmid DNA was prepared using the Wizard Plus DNA purification system from Promega. *C. mixtus* genomic DNA was isolated as described previously (14). The genomic library was constructed in λZAPII using the approach described by Clarke *et al.* (15). The library was plated on NZYM top agar at a density of 3 plaques/cm^2 and was subjected to plaque hybridization using the α-galactosidase gene of *C. mixtus* as the probe.[3] DNA hybridizations were performed using the fluorescein system from Amersham Biosciences according to the manufacturer's protocol. Plasmids (pBluescript SK$^-$) containing genomic DNA inserts from *C. mixtus* were excised from positive recombinant phage and rescued into *E. coli* XL1-Blue, as described in the Stratagene protocol. Two inverse PCR amplifications were performed to clone the full-length sequence of the genes located upstream from *man5A* (encodes *Cm*Man5A). Briefly, for the first inverse PCR experiment, *C. mixtus* genomic DNA was digested with the enzyme EcoRI, and resulting DNA fragments ranging from 4.5 to 5.5 kb were eluted from agarose gels and religated. In the second experiment the enzyme used was PstI, and the fragments that ranged from 1.5 and 2.5 kb were ligated. The primer pairs used in the first and second amplifications were as follows: first amplification (EcoRI), 5′-GCAGGTCCATAAACATACGC-3′ and 5′-GGTTGGCCAATATTTTGCGC-3′; and second amplification (PstI), 5′-CAATGACAGATGAAGGAAGC-3′ and 5′-CTTAGCGCTATTGCTGATTG-3′. PCRs were performed using 1 unit of the thermostable DNA polymerase pFU turbo (Stratagene) and following the manufacturer's instructions. PCR products were cloned into pGEM T-easy (Promega). The nucleotide sequence of DNA was determined with an ABI Prism Ready Reaction DyeDeoxy terminator cycle sequencing kit and Applied Biosystems 377A sequencing system. The complete sequence of the DNA (both strands) was determined using a series of custom made primers. The sequences were compiled and ordered using the computer software DNAsis from Hitachi. Site-directed mutagenesis, employing a QuikChange (Stratagene) kit and appropriate primers, was used to construct mutants of *man5A* that encoded the catalytic acid-base (E215A) and nucleophile (E330A) mutants of *Cm*Man5A.

Expression and Purification of CmMan5A—To express wild type and mutant forms of *Cm*Man5A in *E. coli*, DNA encoding the mature enzyme (residues 26–456) was amplified by PCR from *C mixtus* genomic DNA using the primers 5′-CTC**CATATG**GTTGCAGAAAGTAAC-3′ and 5′-CAC**CTCGAG**TTTCGGCTGAAAACG-3′ (incorporated restriction sites are in bold type) and the thermostable DNA polymerase pFU Turbo. The PCR product was cloned into pGEM T-easy and sequenced to ensure that no mutations had occurred during the amplification. The recombinant of pGEM T-easy containing *man5A* was digested with NdeI and XhoI, and the excised mannosidase gene was cloned into the similarly restricted expression vector pET21a to generate pFD1. *Cm*Man5A encoded by pFD1 contains a C-terminal His_6 tag. *E. coli* BL21 harboring pFD1 was cultured in LB containing 100 μg ml^{-1} ampicillin at 37 °C to mid-exponential phase (A_{550} = 0.6), at which point isopropyl-β-D-thiogalactopyranoside was added to a final concentration of 1 mM and the cultures were incubated for a further 5 h. The cells were collected by centrifugation, and the cell pellet was resuspended in a 50 mM sodium Hepes buffer, pH 7.5, containing 1 M NaCl and 10 mM imidazole. For biochemical assays, recombinant *Cm*Man5A was purified by immobilized metal ion affinity chromatography as described previously (16).

Production and Purification of Seleno-L-methionine Containing CmMan5A—The methionine auxotroph *E. coli* B834 (DE3) transformed with pFD1 was cultured at 37 °C in 1 liter of culture medium as described by Charnock *et al.* (17). *Cm*Man5A expression was induced by the addition of 1 mM isopropyl-β-D-thiogalactopyranoside. Incubation was continued at 37 °C for a further 16 h, after which time the cells were collected, and the recombinant protein was purified by affinity chromatography as described above. For crystallization trials gel filtration was included as a further purification step. Briefly, the enzyme was buffer exchanged, using a PD-10 Sephadex G-25 M gel filtration column (Amersham Biosciences), into 50 mM sodium Hepes buffer, pH 7.5, containing 200 mM NaCl (Buffer A), concentrated to 20 mg ml^{-1} with Amicon 10-kDa molecular mass centrifugation membranes, and subjected to gel filtration using a HiLoad 16/60 Superdex 75 column (Amersham Biosciences) with protein eluted at 1 ml min^{-1} in Buffer A.

TABLE I
Crystal, data, and refinement quality statistics for the Man5A from C. mixtus

Crystal parameters	
Space group	$P2_12_12$
Cell dimensions	
a (Å)	91.2
b (Å)	101.8
c (Å)	50.3
Data quality	
Wavelength (Å)	0.9791
Resolution of data (outer shell) (Å)	19.88–1.5 (1.55–1.5)
Unique reflections	73,917
R_{merge} (outer shell)[a]	0.073 (0.295)
Mean I / σI (outer shell)	20.8 (3.6)
Completeness (outer shell) %	97.8 (81.7)
Multiplicity (outer shell)	6.0 (3.1)
Refinement	
Protein atoms	4121
Solvent waters	644
Ions	3 SO_4
R_{cryst}	0.122
R_{free}	0.151
Root mean square deviation	
1–2 bonds (Å)	0.010
1–3 angles (°)	1.328

[a] $R_{merge} = (\Sigma_{hkl} \Sigma_i I_{hkl} - (I_{hkl}) / \Sigma_{hkl} \Sigma_i [I_{hkl}])$.

[3] C. Fontes, unpublished observation.

TABLE II
Catalytic activity of CmMan5A

Substrate	*Cm*Man5A	k_{cat}/K_m	k_{cat}	K_m
		$min^{-1}\ M^{-1}$	min^{-1}	mM
PNP-β-mannopyranose[a]	Wild type	1.3×10^3	2.0	1.6
Mannobiose	Wild type	1.5×10^5	1.3×10^2	0.9
Mannotriose	Wild type	1.0×10^8	1.0×10^4	0.1
Mannotetraose	Wild type	9.9×10^7	—[b]	—
1-Galactosyl-mannotriose[c]	Wild type	1.1×10^7	—	—
Mannose-β1,4-glucose[d]	Wild type	5.2×10^2	3.17	6.1
Ivory nut mannan	Wild type	90[e]	2.5×10^2	2.8[e]
1,4-β-D-Mannan (d.p. 15)	Wild type	120[e]	3.0×10^2	2.5[e]
1,4-β-D-Mannan (d.p. 15)	E215A	NA[f]	—	—
1,4-β-D-Mannan (d.p. 15)	E330A	NA	—	—
PNP-β-mannopyranose	E215A	535	5.3×10^{-3}	0.1
PNP-β-mannopyranose	E330A	NA	—	—

[a] PNP, 4-nitrophenyl-β-D-linked aryl chromophore.
[b] —, not measured.
[c] α-1,6-Linked galactose side chain on the reducing end of mannotriose. Only one mannose was released per molecule of substrate at the completion of the reaction.
[d] Disaccharide of mannose and glucose with mannose at the nonreducing end.
[e] Rates against polysaccharide substrates quoted as k_{cat}/K_m (min^{-1} mg ml^{-1}) and K_m (mg ml^{-1}).
[f] NA, no activity detected.

Purified enzyme was concentrated, as described before, washed three times with 5 mM dithiothreitol using the same centrifugal membranes, and the final protein concentration was adjusted to 50 mg ml^{-1}. Matrix-assisted laser desorption ionization time-of-flight mass spectrometric analysis confirmed the identity of the polypeptide and indicated that the protein contained 16 internal seleno-L-methionine residues, whereas the N-terminal modified methionine residue had been processed in *E. coli*.

Enzyme Assay—The activity of *Cm*Man5A was determined at 37 °C in 50 mM sodium phosphate buffer, pH 7.0 (pH optimum of the enzyme; data not shown) containing 1 mg ml^{-1} bovine serum albumin and the appropriate substrate. To screen for activity against 4-nitrophenyl-glycosides, substrate and enzyme concentrations were 5 mM and 1 μM, respectively, and assays were carried out for up to 30 min. Apart from the use of a different aryl-glycoside as substrate, determination of the kinetic parameters of *Cm*Man5A against 4-nitrophenyl-β-D-mannopyranoside was essentially as described by Charnock *et al.* (18). To screen for endo-glycanase activity, 100 μg of enzyme in a volume of 20 μl was spotted onto a 2% (w/v) agar plate containing 0.5% of the appropriate dyed polysaccharide in 50 mM sodium phosphate buffer, pH 7.0, and the plates were incubated at 37 °C for 16 h. Activity was denoted by a clear halo surrounding the "enzyme spot." Dionex HPLC was used to determine the reaction products generated and to quantify the release of mannose using the methods of Hogg *et al.* (19). To determine kinetic parameters for mannobiose, substrate concentrations were 0.5–3 times the K_m concentration; however, for longer oligosaccharides substrate concentration was not more than 1.5 times the K_m concentration to minimize transglycosylation. The activity of *Cm*Man5A against ivory nut mannan and degalactosylated carob galactomannan was determined by the Somogyi-Nelson reducing sugar assay (20), although the reaction products were also subjected to HPLC (21) to identify the sugars produced. For each assay several times points were analyzed to ensure that the initial linear rate of the reaction was determined. For substrates where the K_m was higher than the solubility of the substrate k_{cat}/K_m was determined at a minimum of three substrate concentrations to ensure that there was a linear relationship between substrate concentration and catalytic rate.

Isothermal Titration Calorimetry—The inactive catalytic nucleophile and acid-base mutants of *Cm*Man5A, E330A and E215A, respectively, were titrated against mannose, mannobiose, mannotriose, and mannotetraose essentially as described previously (17). The concentration of protein in the cell varied from 150 to 300 μM, and titrations were carried out in 50 mM sodium phosphate buffer, pH 7.0, at 25 °C. The experimentally determined change in enthalpy (ΔH) and the association constant (K_a) for substrate binding were used to calculate the change in entropy (ΔS) and Gibbs free energy (ΔG) employing the following equation: $-RTK_A = \Delta G = \Delta H - T\Delta S$.

Crystallization and Data Collection—Crystals of seleno-L-methionine containing protein were grown by vapor phase diffusion using the hanging drop method with an equal volume (1 μl) of protein (50 mg ml^{-1} in water) and reservoir solution (20–24% PEG 4000, 0.1 M sodium acetate pH 4.6, and 0.2 M ammonium sulfate). The crystals grew over a period of 3–4 days and belong to space group $P2_12_12$, with approximate unit cell dimensions a = 91.2, b = 101.8, and c = 50.3 Å. This corresponds to a solvent content of 46.8% (22), assuming 1 molecule/asymmetric unit.

A single crystal of selenomethionine *Cm*Man5A was transferred from the mother liquor to a stabilizing solution incorporating 25% (v/v) glycerol as cryo-protectant. The crystal was mounted in a rayon loop and flash-cooled to a temperature of 120 K in gaseous N_2. Diffraction was assessed using a home source, and a SAD experiment was conducted on beamline ID29 at the European Synchrotron Radiation Facility (Grenoble, France) at a temperature of 100 K with an ADSC charge-coupled device as detector. The wavelength for the SAD experiment was chosen by scanning through the absorption edge of the crystal, and data were collected at the wavelength corresponding to the maximum f''. The data were integrated, scaled, and reduced using DENZO and SCALEPACK (23) as part of HKL2000, with all further computation using the CCP4 suite of programs (24).

Phasing, Model Building, and Refinement—16 selenium sites were found using the anomalous differences with the program SHELXD (25), corresponding to the methionines present in one molecule. The correlation coefficients between observed and calculated E values output by SHELXD were 47.07 (all data) and 28.70 (weak data). selenium positions were refined, and SAD phases were calculated, using the CCP4 program MLPHARE, giving an overall figure of merit of 0.16. The resulting phases were used as a starting set for phase improvement by solvent flattening in the program DM (26), giving an overall figure of merit of 0.75. DM-improved phases were of sufficient quality to allow subsequent tracing of the entire molecule using REFMAC/ARP/wARP in "warpNtrace" mode (27). The model was refined using the CCP4 program REFMAC (28) with manual correction to the model performed using the X-FIT (29) routines of QUANTA (Accelrys, San Diego, CA). The final model consists of 4121 non-hydrogen protein atoms with 644 water molecules and 3 ions. The crystallographic R factor and R_{free} factor are respectively 12.2% and 15.1% (Table I). The stereochemistry of the model was assessed with the program PROCHECK (30) prior to deposition.

RESULTS

Characterization of the C. mixtus Gene Cluster Containing man5A

The region upstream of the α-galactosidase gene of *C. mixtus* was cloned by a combination of library screening using the α-galactosidase gene as the probe and inverse PCR. The derived sequence comprised an operon (GenBank™ accession number AY526725) containing three genes of 1179, 1230, and 1368 bp designated *unkA*, *pmiA*, and *man5A*, respectively. Southern hybridization using *man5A* as the probe showed that a single copy of the gene is present in the bacterial genome (data not shown). The codon usage of the three genes is similar to that of other *Cellvibrio* enzymes, and the proposed ATG translational start codons are preceded (7–12 bp) by typical

prokaryotic ribosome-binding sequences. A DNA palindromic sequence capable of forming a stem-loop with a ΔG value of 21.7 kcal mol^{-1} followed by an A+T-rich region was present downstream of *man5A*. This structure is characteristic of a Rho-independent transcription terminator sequence.

Comparison of the sequence of the three deduced polypeptides with biological databanks, searched by BLAST (www.ncbi.nlm.nih.gov/BLAST), showed that the protein encoded by *unkA* has 12 homologues with no demonstrated enzymatic function (although all annotated as putative glycosidases), whereas the *pmiA* protein exhibits sequence similarity with *N*-acyl-D-glucosamine-2-epimerases and phosphomannose isomerase.[4] The protein encoded by *man5A,* designated β-mannosidase 5A (*Cm*Man5A), contains a typical Type II signal peptide in which an N-terminal basic residue is followed by 15 small hydrophobic amino acids capable of forming a α-helical structure, with cleavage predicted to occur between Ala^{19} and Cys^{20} and the sulfur-containing amino acid linked to the lipid bilayer. The enzyme is therefore attached to either the inner or outer membrane. It should be noted, however, that other *Cellvibrio* exo-acting glycosidases are located on the outer membrane (31, 32), and it is likely that *Cm*Man5A is also on the extracellular surface of the bacterium. Within this context it is interesting to note that the 21 residues downstream of the signal peptide are disordered in the crystal structure and can be removed without influencing the catalytic activity of the enzyme (data not shown), indicating that this sequence may fulfill a linker function.

*Cm*Man5A displays considerable sequence similarity with GH5 enzymes. The sequence classification of Henrissat and Coutinho (4, 5), however, has further been divided, by others, into subfamilies (33), and *Cm*Man5A appears to be located in subfamily 6 of GH5 (see Fig. S1 in supplementary material). Sequence alignment (Fig. S2 in supplementary material) shows that *Cm*Man5A displays the highest (>43%) identity with putative GH5 mannanases from *Microbulbifer degradans* (ZP_00065642) and *Caulobacter crescentus* (AE005756). Interestingly, both enzymes contain the key structural elements that are predicted to confer exo activity (described below). Thus, the *Microbulbifer* and *Caulobacter* proteins lack the asparagine that plays a key role in mannose recognition at the −2 subsite and contain the tryptophan residue and the extended loop between strand β8 and helix α8 that block substrate access to the glycone region of the active site that is distal to the −1 subsite. We therefore predict that the GH5 *Microbulbifer* and *Caulobacter* enzymes will both display β-mannosidase activity.

Biochemical Properties of CmMan5A

CmMan5A Hydrolyzes Mannose-containing Substrates—Purified *Cm*Man5A hydrolyzes aryl-β-mannosides but does not exhibit any activity against aryl-α-mannosides, 4-nitrophenyl-β-glucopyranoside, aryl-α-glucosides, aryl-β-xylopyranosides, aryl-β-galactopyranoside, or aryl-β-arabinosides (Table II). The enzyme does not hydrolyze arabinans, galactans xylans, pectins, cellulose, or soluble cellulosic derivatives and appears not to display endo-β1,4-mannanase activity because it does not release dyed oligosaccharides from azo-carob galactomannan. *Cm*Man5A releases reducing sugar from ivory nut mannan and degalactosylated carob galactomannan (Table II), with mannose the only soluble product produced from these *manno*-configured substrates (Fig. 2). Interestingly, the enzyme displays a similar level of activity against all of these insoluble substrates, which is in sharp contrast to the *Cellvibrio* mannanases that generally exhibit little or no activity against crystalline mannans but are active against the more amorphous degalactosylated carob galactomannan (19). The glycoside hydrolase exhibits limited activity against glucomannan and carob galactomannan, but again mannose is the only low molecular mass reaction product evident (Fig. 3). *Cm*Man5A displays much higher activity against mannooligosaccharides than soluble or insoluble mannose-containing polysaccharides, with a d.p. of >2 (Table II). The enzyme exhibits similar activity against mannotriose and mannotetraose, hydrolyzes mannobiose slowly, displays very low activity against mannose-β-1,4-glucose, and is completely inactive against glucose-β-1,4-mannose. At low substrate concentrations, during the initial stages of the reactions, mannose and a oligosaccharides with a d.p. of $n - 1$ (where the d.p. of the substrate is n) are the only reaction products evident. At high concentrations of the substrates mannotriose and mannotetraose, oligosaccharides with d.p. values larger than 3 and 4, respectively, were generated during the initial phase of the reactions, indicating that the glycoside hydrolase is able to catalyze transglycosylation as well as hydrolysis. This is consistent with a double displacement mechanism, which is displayed by all GH5 enzymes characterized to date (34, 35). The lack of larger products when mannobiose is the substrate reflects the significantly higher activity of the enzyme against trisaccharides compared with disaccharides; oligosaccharides with d.p. values of >2 would be

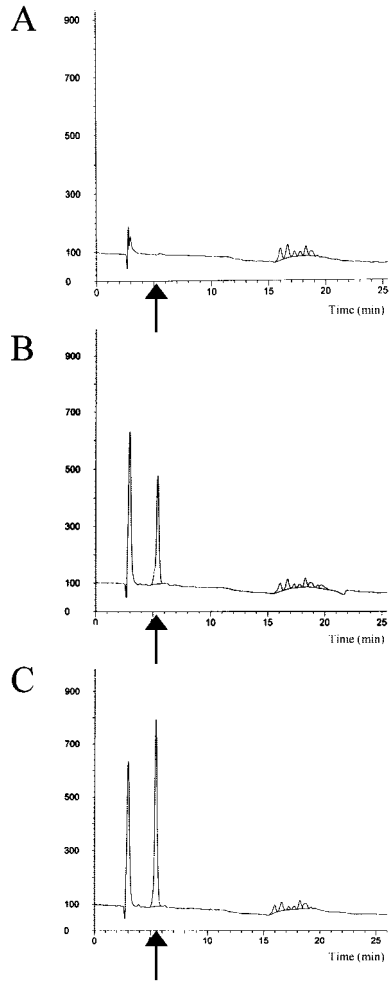

FIG. 2. **HPLC analysis of reaction products of *Cm*Man5A against 1,4-β-D-Mannan.** Hydrolysis of insoluble 1,4-β-D-mannan (2 mg/ml) by *Cm*Man5A (1.0 μM). *A–C* show the times 0, 1, and 5 min, respectively. The *arrow* in each panel indicates the retention time of mannose under the elution gradient used.

[4] F. M. V. Dias, F. Vincent, G. Pell, J. A. M. Prates, M. S. J. Centeno, L. E. Tailford, L. M. A. Ferreira, C. M. G. A. Fontes, G. J. Davies, and H. J. Gilbert, manuscript in preparation.

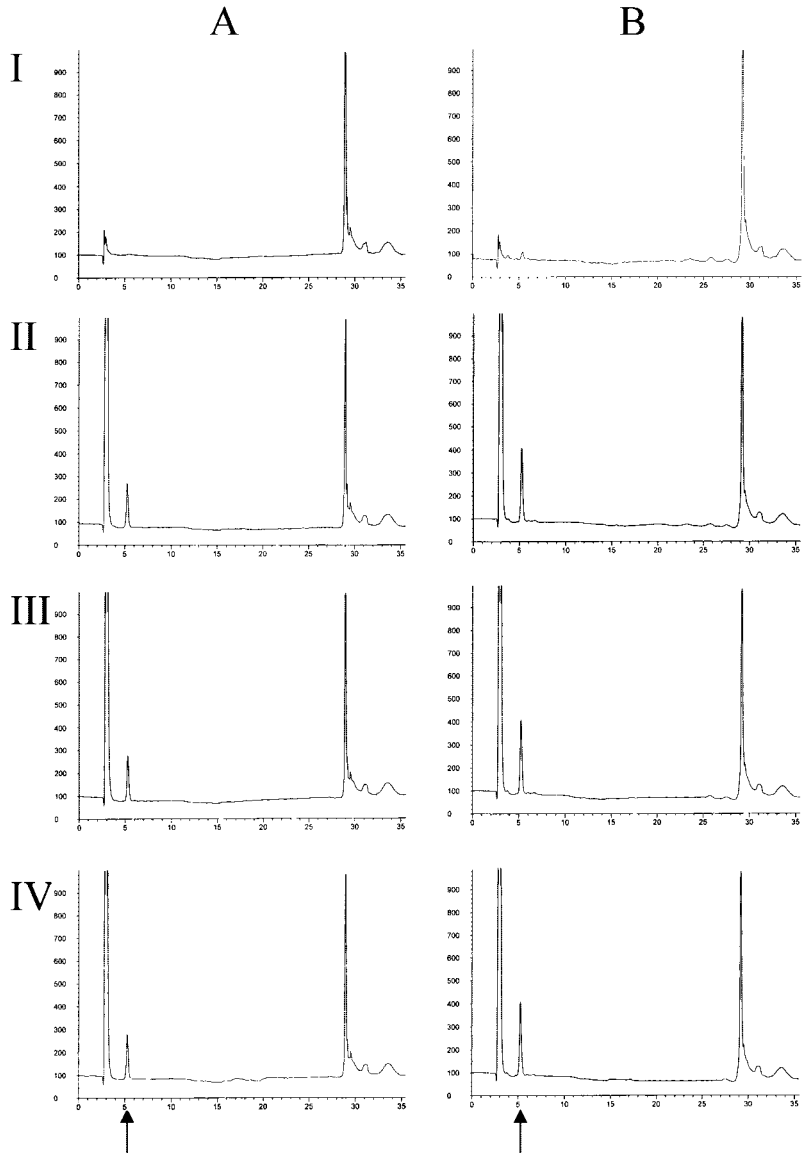

FIG. 3. **Limited hydrolysis of galactomannan and glucomannan by *Cm*Man5A.** HPLC traces showing hydrolysis of galactomannan (*A*) and glucomannan (*B*) by 10 μM *Cm*Man5A, at the times 0 min, 1 min, 5 min, and 18 h for *panels I–IV*, respectively. The *arrows* indicate the retention time of mannose.

hydrolyzed much more quickly than mannobiose and thus do not accumulate.

The data described above indicate that *Cm*Man5A is an exo-acting mannanase, or β-mannosidase (the distinction between these two activities is rather diffuse). The enzyme contains two kinetically significant aglycone sugar-binding subsites, defined as +1 and +2, and a single glycone-binding site designated subsite −1. The ΔG for substrate binding at the +2 subsite, determined by the method of Suganuma *et al.* (36), is 3.6 kcal mol^{-1}. The −1 subsite displays absolute specificity for manno-configured substrates, whereas the +1 subsite exhibits a strong preference for mannose, although it will interact weakly with glucose; the difference in the ΔG for binding the two sugars at this location is 3.5 kcal mol^{-1}. The weak binding of glucose at the +1 subsite may result from a steric clash between the O_2 equatorial hydroxyl of the sugar with the protein, or the enzyme may make important hydrogen bonds with the axial O_2 of mannose but not with the equivalent group in glucose. The properties of *Cm*Man5A are not typical of GH1 or GH2 β-mannosidases, which have been shown not to attack insoluble mannan and instead typically display maximum activity against aryl-mannosides as exemplified by *C. fimi* Man2A, which has a k_{cat}/K_m value ~25,000-fold greater than *Cm*Man5A for 4-nitrophenyl-β-D-mannopyranoside (8). GH1 and GH2 mannosidases also often exhibit product inhibition at substrate concentrations as low as 400 μM (8), whereas only very high concentrations of mannose (K_i = ~400 mM) inhibit *Cm*Man5A. Man-6-P inhibits with a K_i if ~30 mM, suggesting that phosphorylated ligands are also accommodated, but the pattern of inhibition is noncompetitive, and so the catalytic relevance of this observation is unclear. *Cm*Man5A contains +1 and +2 subsites that bind strongly to *manno*-configured substrates, and it is unclear whether the mannosidases, glucosidases, and xylosidases in GH1 and GH2 also display tight specificity for the aglycone region of their target substrates.

CmMan5A Can Accommodate Decorated Mannosyl Residues at the +2 Subsite—The capacity of *Cm*Man5A to hydrolyze α-1,6-galactose-decorated mannooligosaccharides was also determined by HPLC. Hydrolysis of 1-galactosyl-mannotriose by *Cm*Man5A released only a single mannose per substrate molecule, and the enzyme displayed no activity against 3,4-digalactosyl-mannopentaose (data not shown). These data indicate that *Cm*Man5A can accommodate a galactose side chain in the +2 subsite, but the reduced, ~9-fold, lower activity of 1-galactosyl-mannotriose compared with undecorated mannotriose indicates that the side chain is likely to form a steric clash with the enzyme at this location (Table II). Because only a single mannose is released from 1-galactosyl-mannotriose, the reac-

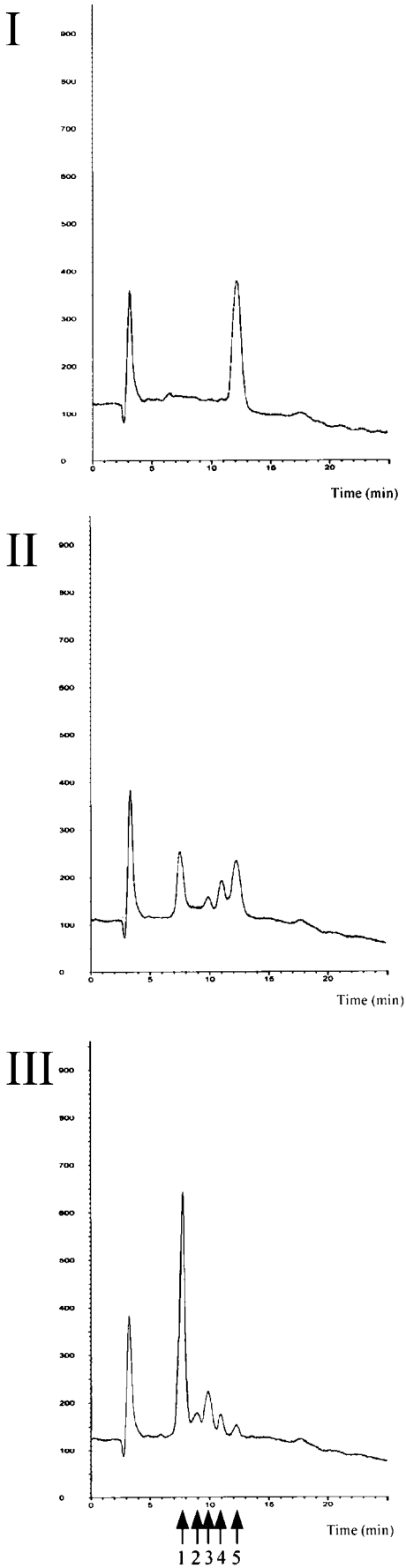

FIG. 4. **Reaction products generated by the hydrolysis of reduced mannohexaose by *Cj*Man5C and *Cm*Man5A.** *A* shows the hydrolysis of mannohexitol (3 μg/ml) by 4 nM *Cm*Man5A. The reactions were analyzed after 0 min (*panel I*), 10 min (*panel II*), and 30 min (*panel III*). *Arrow 1*, mannose; *arrow 2*, mannotritol; *arrow 3*, mannotetritol; *arrow 4*, mannopentitol; *arrow 5*, mannohexitol. The peaks were unambiguously identified by spiking the reaction products with standard sugars and sugar alditols and reanalyzing them by HPLC (data not shown). Each reaction was analyzed using two different HPLC elution gradient protocols, because it proved impossible to achieve a single gradient in which none of the sugars and sugar alditols co-eluted. The data shown for each reaction is an HPLC protocol (isocratic in 12.5 mM sodium hydroxide) in which none of the products of that particular reaction co-eluted.

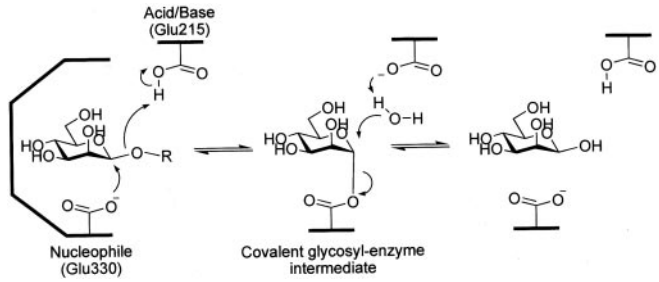

FIG. 5. **Reaction mechanism for *Cm*Man5.** Catalysis is performed with net retention of anomeric configuration through a covalent glycosyl-enzyme intermediate.

tion product 1-galactosyl-mannobiose is not further hydrolyzed, and the enzyme is thus unable to accommodate the sugar side chain in the +1 subsite. The complete lack of hydrolysis of 3,4-digalactosyl-mannopentaose supports the view that only unsubstituted mannose residues can be accommodated at the +1 subsite.

CmMan5A Attacks the Nonreducing Ends of Substrates—To establish whether *Cm*Man5A releases mannose from the reducing or nonreducing end of mannooligosaccharides, mannohexaose was converted into the alditol (mannohexitol) by treatment with sodium borohydride. The hydrolysis products of reduced mannohexaose could be distinguished by the differing elution times of the sugar alditols from native manno-oligosaccharides using HPLC. Initial hydrolysis products (Fig. 4) are mannose and manno-oligosaccharide alditols with d.p. values from three to five (mannotritol, mannotetritol and mannopentitol). The initial rate of hydrolysis of M6-R was indistinguishable from that of mannohexaose (data not shown), demonstrating that *Cm*Man5A releases β-1,4-linked mannose substrates exclusively from the nonreducing end.

Identification of the Catalytic Residues of CmMan5A

The location of *Cm*Man5A in GH5 indicates that the enzyme performs catalysis with net retention of anomeric configuration through a covalent glycosyl-enzyme intermediate (Fig. 5). Comparison of the primary sequence of *Cm*Man5A with other GH5 members indicates that Glu^{215} and Glu^{330} align with residues that have been shown to act as the catalytic acid-base and catalytic nucleophile respectively, in selected GH5 enzymes (7). This view is supported by the location of these two amino acids in the three-dimensional structure of *Cm*Man5A (described below). To investigate the proposed role of the two glutamates, these residues were replaced by alanine, and the biochemical properties of the resultant mutants, E215A and E330A, were analyzed. E330A displays no activity against mannan or 4-nitrophenyl-β-mannopyranoside, supporting the view that Glu^{330} is the catalytic nucleophile. Although E215A also exhibits no activity against mannan, it is active against 4-nitrophenyl-β-mannopyranoside, and this activity is accompanied by a significant decrease in K_m. The properties of E215A are entirely consistent with the loss of the acid-base catalytic residue, because such mutants can cata-

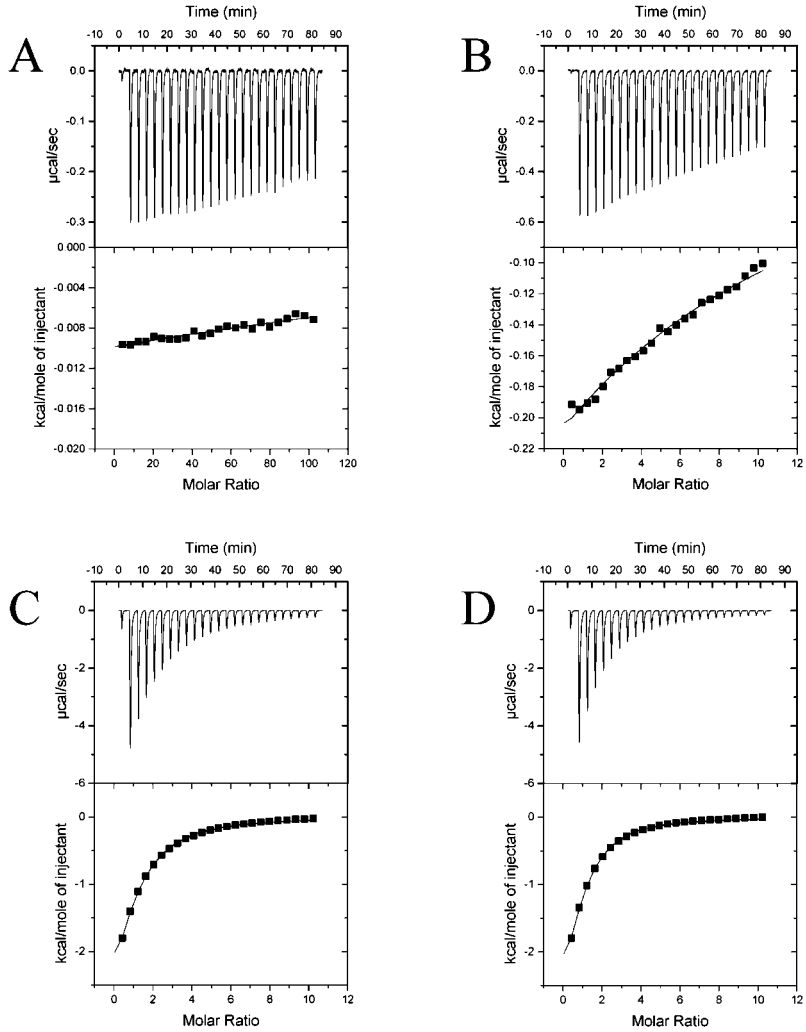

FIG. 6. **Typical ITC titrations of the inactive *Cm*Man5A mutants with manno-oligosaccharides.** *Cm*Man5A E330S (177 μM in 50 mM sodium phosphate buffer) titrated with mannose (*A*, 100 mM), mannobiose (*B*, 10 mM), mannotriose (*C*, 10 mM), and mannotetraose (*D*, 10 mM). The *top section* of each panel shows the raw heats of binding, and the *bottom section* shows the integrated heats, fitted by nonlinear regression analysis to a single site binding model.

TABLE III
Affinity of CmMan5A wild type and inactive mutants for mannooligosaccharides as determined by ITC

Protein	Ligand	K_a	ΔG	ΔH	$T\Delta S$	n
		M^{-1}	kcal mol^{-1}	kcal mol^{-1}	kcal mol^{-1}	
Wild type	Mannose[a]	0.45 ± 0.81	—[b]	—	—	1.0 ± 0.0[c]
E330S	Mannose[a]	0.21 ± 0.7	—	—	—	1.0 ± 0.0[c]
E330S	Mannobiose[a]	118.8 ± 6.0	—	—	—	1.0 ± 0.0[c]
E330S	Mannotriose	4442.0 ± 230.9	−5.0 ± 0.2	−4.7 ± 0.3	0.3 ± 0.1	0.97 ± 0.1
E330S	Mannotetraose	6548.0 ± 406.8	−5.2 ± 0.2	−3.9 ± 0.3	1.3 ± 0.2	0.93 ± 0.2
E215A	Mannose[a]	11.3 ± 1.4	—	—	—	1.0 ± 0.0[c]
E215A	Mannobiose[a]	210.4 ± 11.9	—	—	—	1.0 ± 0.0[c]
E215A	Mannotriose	18070.0 ± 302.8	−5.8 ± 0.0	−12.0 ± 0.1	−6.3 ± 0.1	0.99 ± 0.0
E215A	Mannotetraose	34800.0 ± 743.0	−6.2 ± 0.1	−12.1 ± 0.1	−6.0 ± 0.1	0.95 ± 0.0

[a] An estimate of the affinity is given, because the affinity is below the range for accurate determination.
[b] —, not calculated.
[c] n fixed at 1 for the purposes of fitting data, because the affinities were below the level for accurate determination of binding stoichiometry.

lyze glycosidic bond cleavage of substrates that contain reasonable leaving groups, such as the aryl-mannoside, but deglycosylate very poorly leading to the accumulation of a covalent enzyme-product complex and a decrease in K_m (18, 37).

The Use of ITC to Estimate the Number of Subsites in CmMan5A

In an alternative approach to determining the number of sugar-binding sites, the affinity for mannooligosaccharides of inactive mutants lacking either the catalytic acid-base (E215A) or the catalytic nucleophile (E330A) was determined by ITC (Fig. 6 and Table III). The K_a for mannotriose and mannotetraose are very similar, consistent with the view that the enzyme contains only three sugar-binding sites. The ~30–90-fold lower affinity for mannobiose compared with the trisaccharide is in agreement with the large increase in catalytic efficiency displayed by mannotriose compared with the disaccharide. The weak affinity of both mutants and the wild type enzyme for mannose demonstrates why the monosaccharide acts as an extremely poor competitive inhibitor. The affinity constants derived from the binding of mannooligosaccharides to inactive enzyme and the catalytic efficiency of the mannosidase against different mannose polymers, respectively, indicate that the

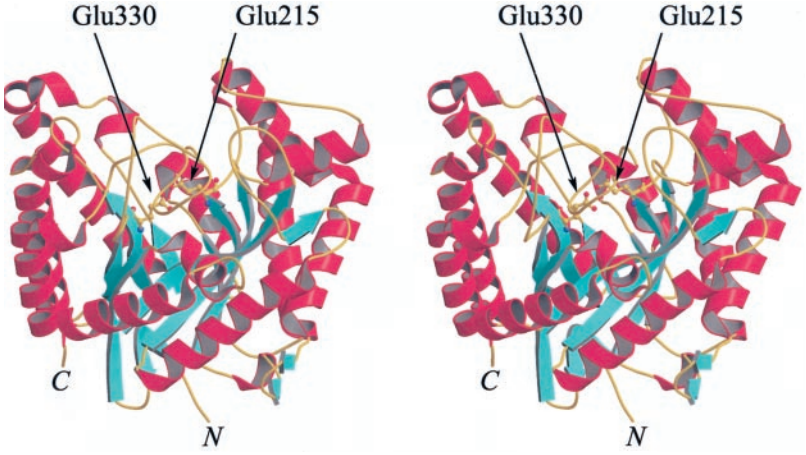

FIG. 7. **Three-dimensional structure of the *C. mixtus* exo-β-mannosidase *Cm*Man5A.** Shown is a protein cartoon of the *Cm*Man5A structure in divergent wall-eyed stereo. The catalytic acid/base and nucleophile, Glu^{215} and Glu^{330}, are shown in "ball-and-stick" representation. *Cm*Man5A is a typical GH-A clan member (7) This figure was drawn with MOLSCRIPT (45).

enzyme contains three sugar-binding subsites, −1 to +2. The absolute affinities derived from the binding of the inactive forms of *Cm*Man5A to substrates, however, must be treated with some caution because the effect on binding efficiency of the loss of interactions between the sugar polymers and the catalytic nucleophile and acid-base residues, respectively, is unknown.

Crystal Structure of CmMan5A

The structure of *CmMan5* was solved using the SAD methods with seleno-L-methionine protein and refined at 1.5 Å resolution (Table I) (Protein Data Bank identification code 1uuq). The polypeptide chain is visible from residue 20 (Glu^{44} in the full-length enzyme) through to 431, with both the N-terminal 21 amino acids and the C-terminal histidine tag not visible in electron density. In addition, three sulfate ions and three glycerol molecules have been included in refinement. As expected for a GH5 glycosidase, *Cm*Man5 displays the $(\beta/\alpha)_8$ barrel architecture (residues 41–428) and presents the putative acid-base, Glu^{215}, and the catalytic nucleophile, Glu^{330}, at the end the β-strands 4 and 7, respectively (Fig. 7).

The structure of *Cm*Man5A shows a high degree of similarity with the endo-mannanases from this family. The superposition of *Cm*Man5A with the endo β-mannanase from *Hypocrea jecorina* (formerly known as *Trichoderma reesei*), designated *Hj*Man5A, (38) shows that the β barrel architecture is highly conserved with a root mean square deviation of 1.3 Å for 286 equivalent Cα atom using LSQMAN (39) (Fig. 8*a*). Additionally, the N-terminal segment of *Cm*Man5A (residues 22–40), as with *Hj*Man5A, forms a small two-stranded β-sheet sealing the bottom of the β barrel. In addition to the catalytic residues, *Cm*Man5A contains several key residues that have been identified as "strictly conserved" in family GH5 (40). The following residues in *Cm*Man5A superimpose with amino acids in *Hj*Man5A (the *Hj*Man5A residues are shown in parentheses): Arg^{80} (Arg^{54}), Asn^{214} (Asn^{168}), Glu^{215} (Glu^{169}), His^{283} (His^{241}), Glu^{330} (Glu^{276}), and Trp^{376} (Trp^{306}). The catalytic acid-base, Glu^{215}, forms hydrogen bonds with Arg^{80} and His^{383}, and these interactions are likely to contribute to both the position and ionization state of this critical amino acid. Asn^{214}, whose orientation is stabilized through a hydrogen bond with Arg^{80}, is highly conserved in clan GH-A glycoside hydrolases and plays an important role in transition state stabilization by making a hydrogen bond with the O_2 of the sugar at the −1 subsite (18, 41). The position of the catalytic nucleophile, Glu^{330}, is stabilized through a hydrogen bond with Trp^{285}, whereas Trp^{376}, based upon comparison with other related hydrolases, is likely to form the hydrophobic sugar-binding platform in subsite −1.

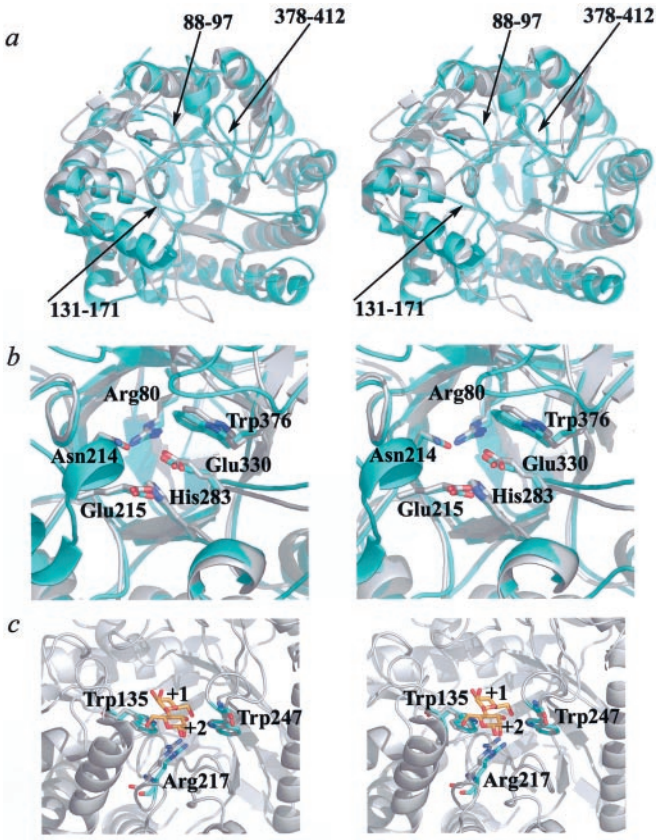

FIG. 8. **Comparison of the *C. mixtus* exo-β-mannosidase CmMan5A (*cyan*) with the endo-acting GH5 mannanase (*gray*) from *H. jecorina* (*T. reesei*).** *a*, three-dimensional structural overlap indicating the three extended loops in CmMan5 that contribute to the enclosure of a pocket active center. The two conserved strands, mentioned in the text, that enclose the center of the C terminus of the β barrel are clear. *b*, structural identity in the active center. *c*, structural conservation in the aglycone region. This figure, in divergent wall-eyed stereo, was drawn with PyMOL (DeLano Scientific, pymol.sourceforge.net/).

Structural Basis for the exo Activity of CmMan5A

The superimposition of the endo and exo mannanase reveals dramatic differences in the length of three loops that modify the active center accessibility and thus modulate the specificity from endo to exo. The most striking and significant of these loop differences is the extended sequence between strand β8 and helix α8 comprising residues 378–412. This insertion forms a "double" steric barrier, formed by two short β-strands that function to "block" the active center at the edge of the −1

subsite, forming the "exo" active center of *Cm*Man5A. In the *H. jecorina* endo-mannanase the equivalent loop is both shorter and, more significantly, folded back by ~90°, which both opens up the active center and forms the base of the glycone-binding subsites (Fig. 8*a*). It is interesting to note that despite steric exclusion of substrate from the distal glycone subsites of *Cm*Man5A, the enzyme retains the two aromatic residues that, in *Thermobifida fusca* mannanase 5A (*Tf*Man5A), interact with substrate at the −3 subsite, however, the asparagine in *Tf*Man5A that makes a hydrogen bond with the −2 sugar is not conserved in the *Cellvibrio* enzyme (Fig. S2 in supplementary material) (40).

In the active center three residues appear to contribute to the recognition of the nonreducing end of the polymer. Gln^{403} and Glu^{404}, derived from the loop described above, lie at the extreme nonreducing end of this tunnel and from analogy with endo-acting GH5 enzymes are likely to interact with O-4 and O-6, respectively, of the mannose residue located at the −1 subsite. A loop insertion between strand β2 and helix α2 (residues 88–97) contributes to the enclosure of the opposite wall of the active center cavity to the 378–412 loop, whereas the "pocket" nature of the center, giving rise to its true exo activity, is derived from the additional steric blockage provided by the loop between β3 and α3 (residues 131–171). This latter loop, which forms three small helical loops (two of which are not present in *Hj*Man5A) donates Trp^{137}, which not only provides the main steric blockage but may also hydrogen bond to O-3 of the sugar at the −1 subsite (based upon the similar interaction mediated by an invariant histidine in many GH-A clan enzymes). More detailed analysis awaits complex data that have not yet been forthcoming.

In the aglycone (leaving group) subsites, the endo and exo mannanase are extremely similar. The structure of *Hj*Man5A has been solved in complex with mannobiose bound at subsites +1 and +2 (38). The residues involved in the interaction with the disaccharide are all present in *Cm*Man5A, with Trp^{135} (+1 subsite), Trp^{289} (+2 subsite), and Arg^{217} (+2 subsite) in *Cm*Man5A corresponding to Trp^{114}, Trp^{247}, and Arg^{171} in *Hj*Man5A, respectively (Fig. 8*b*). This provides a structural basis for the observations that *Cm*Man5A is an exo-mannanase as opposed to a mannosidase and that energy from subsites other than −1 and +1 is required for efficient catalysis.

At the extreme reducing end of the glycone subsites, further differences manifest themselves. The loop from 259 to 267 (connecting β5 with α5) is much shorter in *Cm*Man5A than in the corresponding endo-mannanases (the spatially equivalent loop between β5 and α5 is 20 residues in *Hj*Man5A), which makes the substrate-binding channel more open for the exo-mannanase then observed previously.

The Role of CmMan5A in Cellvibrio

*Cm*Man5A is most likely either located within the periplasm (attached to the inner membrane) or on the surface (attached to the outer membrane) of *C. mixtus* and displays activity against both insoluble and soluble polysaccharides as well as mannooligosaccharides. All of these substrates are available to the enzyme if it is located on the outer membrane. *Cm*Man5A, however, does not contain any associated carbohydrate-binding modules, which are invariably present in glycoside hydrolases that target insoluble substrates (42, 43), indicating that the most probable function of the mannosidase is to hydrolyze shorter mannooligosaccharides released from polymeric insoluble mannans by the repertoire of extracellular endo-mannanases produced by *Cellvibrio* (19). This view is supported by the observation that the enzyme displays much higher activity against mannooligosaccharides with d.p. values of >2 than against decorated soluble polysaccharides or insoluble mannans. A possible biological rationale for the membrane location of *Cm*Man5A is that the mannose and mannobiose released by the enzyme would be generated at the surface of the bacterium and are thus available for preferential uptake by *C. mixtus* rather than competing microorganisms within the milieu of the plant cell wall. The *C. mixtus* Man5A thus provides another example of evolution modifying the loop regions surrounding the active center cleft to change a cleft into a pocket, as first described for the *Candida* β-1,3 glucanase by Cutfield and colleagues (44) to generate beneficial exo-hydrolase activity for the organism. Further genome sequencing will reveal an increasing number of these examples that may now more easily be placed on a three-dimensional foundation.

REFERENCES

1. Brett, C. T., and Waldren, K. (1996) in *Physiology and Biochemistry of Plant Cell Walls: Topics in Plant Functional Biology* (Black, M., and Charlewood, B., eds) Chapman and Hall, London
2. McCleary, B. V. (1988) *Methods Enzymol.* **160,** 523–527
3. Halstead, J. R., Fransen, M. P., Eberhart, R. Y., Park, A. J., Gilbert, H. J., and Hazlewood, G. P. (2000) *FEMS Microbiol. Lett.* **192,** 197–203
4. Henrissat, B. (1991) *Biochem. J.* **280,** 309–316
5. Coutinho, P. M., and Henrissat, B. (1999) in *Recent Advances in Carbohydrate Bioengineering* (Gilbert, J. J., Davies, G., Henrissat, B., and Svensson, B., eds) pp. 3–12, The Royal Society of Chemistry, Cambridge
6. Kempton, J. B., and Withers, S. G. (1992) *Biochemistry* **31,** 9961–9969
7. Henrissat, B., Callebaut, I., Fabrega, S., Lehn, P., Mornon, J. P., and Davies, G. (1995) *Proc. Natl. Acad. Sci. U. S. A.* **92,** 7090–7094
8. Zechel, D. L., Reid, S. P., Stoll, D., Nashiru, O., Warren, R. A., and Withers, S. G. (2003) *Biochemistry* **42,** 7195–7204
9. Stoll, D., He, S., Withers, S. G., and Warren, R. A. (2000) *Biochem. J.* **351,** 833–838
10. McCleary, B. V., and Matheson, N. K. (1986) Adv. *Carbohydr. Chem. Biochem.* **44,** 147–276
11. McCleary, B. V. (1983) *Carbohydr. Res.* **111,** 297–310
12. Millward-Sadler, S. J., Davidson, K., Hazlewood, G. P., Black, G. W., Gilbert, H. J., and Clarke, J. H. (1995) *Biochem. J.* **312,** 39–48
13. Sambrook, J., Fritsch, E. F., and Maniatis, T. (1989) *Molecular Cloning: A Laboratory Manual*, 2nd Ed., Cold Spring Harbor Laboratory, Cold Spring Harbor, New York
14. Berns, K. I., and Thomas, C. A., Jr. (1965) *J. Mol. Biol.* **11,** 476–490
15. Clarke, J. H., Laurie, J. I., Gilbert, H. J., and Hazlewood, G. P. (1991) *FEMS Microbiol. Lett.* **67,** 305–309
16. Xie, H., Bolam, D. N., Nagy, T., Szabo, L., Cooper, A., Simpson, P. J., Lakey, J. H., Williamson, M. P., and Gilbert, H. J. (2001) *Biochemistry* **40,** 5700–5707
17. Charnock, S. J., Bolam, D. N., Turkenburg, J. P., Gilbert, H. J., Ferreira, L. M., Davies, G. J., and Fontes, C. M. (2000) *Biochemistry* **39,** 5013–5021
18. Charnock, S. J., Lakey, J. H., Virden, R., Hughes, N., Sinnott, M. L., Hazlewood, G. P., Pickersgill, R., and Gilbert, H. J. (1997) *J. Biol. Chem.* **272,** 2942–2951
19. Hogg, D., Pell, G., Dupree, P., Goubet, F., Martin-Orue, S. M., Armand, S., and Gilbert, H. J. (2003) *Biochem. J.* **371,** 1027–1043
20. Somogyi, M. (1952) *J. Biol. Chem.* **195,** 19–23
21. Hogg, D., Woo, E. J., Bolam, D. N., McKie, V. A., Gilbert, H. J., and Pickersgill, R. W. (2001) *J. Biol. Chem.* **276,** 31186–31192
22. Matthews, B. W. (1968) *J. Mol. Biol.* **33,** 491–497
23. Otwinowski, Z., and Minor, W. (1997) *Methods Enzymol.* **276,** 307–326
24. Collaborative Computational Project Number 4 (1994) *Acta Crystallogr. Sect. D Biol. Crystallogr.* **50,** 760–763
25. Schneider, T. R., and Sheldrick, G. M. (2002) *Acta Crystallogr. Sect. D Biol. Crystallogr.* **58,** 1772–1779
26. Cowtan, K. D., and Main, P. (1996) *Acta Crystallogr. Sect. D Biol. Crystallogr.* **49,** 148–157
27. Perrakis, A., Morris, R., and Lamzin, V. S. (1999) *Nat. Struct. Biol.* **6,** 458–463
28. Murshudov, G. N., Vagin, A. A., and Dodson, E. J. (1997) *Acta Crystallogr. Sect. D Biol. Crystallogr.* **53,** 240–255
29. Oldfield, T. J. (2001) *Acta Crystallogr. Sect. D Biol. Crystallogr.* **57,** 82–94
30. Laskowski, R. A., McArthur, M. W., Moss, D. S., and Thornton, J. M. (1993) *J. Appl. Crystallogr.* **26,** 282–291
31. Beylot, M. H., Emami, K., McKie, V. A., Gilbert, H. J., and Pell, G. (2001) *Biochem. J.* **358,** 599–605
32. Nagy, T., Emami, K., Fontes, C. M., Ferreira, L. M., Humphry, D. R., and Gilbert, H. J. (2002) *J. Bacteriol.* **184,** 4925–4929
33. Wang, Q., Tull, D., Meinke, A., Gilkes, N. R., Warren, R. A., Aebersold, R., and Withers, S. G. (1993) *J. Biol. Chem.* **268,** 14096–14102
34. Gebler, J., Gilkes, N. R., Claeyssens, M., Wilson, D. B., Beguin, P., Wakarchuk, W. W., Kilburn, D. G., Miller, R. C., Jr., Warren, R. A., and Withers, S. G. (1992) *J. Biol. Chem.* **267,** 12559–12561
35. Davies, G. J., Mackenzie, L., Varrot, A., Dauter, M., Brzozowski, A. M., Schulein, M., and Withers, S. G. (1998) *J. Biol. Chem.* **37,** 11707–11713
36. Suganuma, T., Matsuno, R., Ohnishi, M., and Hiromi, K. (1978) *J. Biochem.* (*Tokyo*) **84,** 293–316
37. MacLeod, A. M., Lindhorst, T., Withers, S. G., and Warren, R. A. (1994)

Biochemistry **33,** 6371–6376
38. Sabini, E., Schubert, H., Murshudov, G., Wilson, K. S., Siika-Aho, M., and Penttilä, M. (1999) *Acta Crystallogr. Sect. D Biol. Crystallogr.* **56,** 3–13
39. Kleywegt, G. J., and Jones, T. A. (1994) *ESF/CCP4 Newsletter* **31,** 9–14
40. Hilge, M., Gloor, S. M., Rypniewski, W., Sauer, O., Heightman, T. D., Zimmermann, W., Winterhalter, K., and Piontek, K. (1998) *Structure* **6,** 1433–1444
41. Williams, S. J., Notenboom, V., Wicki, J., Rose, D. R., and Withers, S. G. (2000) *J. Am. Chem. Soc.* **122,** 4229–4230
42. Boraston, A. B., Revett, T. J., Boraston, C. M., Nurizzo, D., and Davies, G. J. (2003) *Structure* **11,** 665–675
43. Bolam, D. N., Xie, H., White, P., Simpson, P. J., Hancock, S. M., Williamson, M. P., and Gilbert, H. J. (2001) *Biochemistry* **40,** 2468–2477
44. Cutfield, S. M., Davies, G. J., Murshudov, G., Anderson, B. F., Moody, P. C., Sullivan, P. A., and Cutfield, J. F. (1999) *J. Mol. Biol.* **294,** 771–783
45. Kraulis, P. J. (1991) *J. Appl. Crystalogr.* **24,** 946–950